



Diesel exhaust particle exposure causes redistribution of endothelial tube VE-cadherin

Ming-Wei Chao^a, John Kozlosky^b, Iris P. Po^a, Pamela Ohman Strickland^c,
Kathy K.H. Svoboda^d, Keith Cooper^e, Robert J. Laumbach^f, Marion K. Gordon^{a,*}

^a Pharmacology and Toxicology, Rutgers University, Piscataway, NJ 08854, United States

^b Environmental Sciences, Rutgers University, New Brunswick, NJ 08901, United States

^c Family Medicine and Biostatistics, UMDNJ, Robert Wood Johnson Medical School, School of Public Health, Piscataway, NJ 08854, United States

^d Biomedical Science, Baylor College of Dentistry, Texas A&M Health Sciences Center, Dallas, TX 75246, United States

^e Biochemistry and Microbiology, Cook Campus, Rutgers University, New Brunswick, NJ 08901, United States

^f Environmental and Occupational Medicine, UMDNJ, Robert Wood Johnson Medical School, Piscataway, NJ 08854, United States

ARTICLE INFO

Article history:

Received 22 June 2009

Received in revised form 7 September 2010

Accepted 21 September 2010

Available online 29 September 2010

Keywords:

VE-cadherin

Endothelial cells

Endothelial tubes

HUVECs

Diesel exhaust particles

ABSTRACT

Whether diesel exhaust particles (DEPs) potentially have a direct effect on capillary endothelia was examined by following the adherens junction component, vascular endothelial cell cadherin (VE-cadherin). This molecule is incorporated into endothelial adherens junctions at the cell surface, where it forms homodimeric associations with adjacent cells and contributes to the barrier function of the vasculature (Dejana et al., 2008; Venkiteswaran et al., 2002; Villasante et al., 2007). Human umbilical vein endothelial cells (HUVECs) that were pre-formed into capillary-like tube networks *in vitro* were exposed to DEPs for 24 h. After exposure, the integrity of VE-cadherin in adherens junctions was assessed by immunofluorescence analysis, and demonstrated that increasing concentrations of DEPs caused increasing redistribution of VE-cadherin away from the cell–cell junctions toward intracellular locations. Since HUVEC tube networks are three-dimensional structures, whether particles entered the endothelial cells or tubular lumens was also examined. The data indicate that translocation of the particles does occur. The results, obtained in a setting that removes the confounding effects of inflammatory cells or blood components, suggest that if DEPs encounter alveolar capillaries *in vivo*, they may be able to directly affect the endothelial cell–cell junctions.

© 2010 Elsevier Ireland Ltd. All rights reserved.

1. Introduction

Epidemiological studies demonstrate an association between short-term increases in ambient air particulates and adverse cardiovascular events within a 48 h timespan, especially in the elderly or those with pre-existing coronary artery disease (Peters et al., 2001a,b, 2004; Pope and Dockery, 2006; Zanobetti and Schwartz, 2005). Vascular dysfunction is one of the potential mechanisms that may mediate the cardiovascular effects of exposure to particulate matter. Impaired endothelial-dependent vasodilation occurs in healthy young adults exercising near roadways (Rundell et al.,

2007) and in older adults exposed to traffic at bus stops (Dales et al., 2007). Groups with pre-existing vascular dysfunction, such as diabetics (O'Neill et al., 2005), have an increased susceptibility to exposure to ambient particulate matter, and an exacerbated inflammatory response is observed in those with non-functional phase II enzyme variants (Gilliland et al., 2004). In addition to the lung's inflammatory response, pulmonary edema has been noted from exposure to particulates (Inoue et al., 2006; Nemmar et al., 2007; Sagai et al., 1993; Singh et al., 2004), indicating increased pulmonary vascular permeability. The presence of microalbumin in bronchoalveolar lavage fluid also supports the observation of vascular leakage into the lung. This can occur as early as 4 h after exposure, as shown in mice who involuntarily aspirated automobile DEPs (Singh et al., 2004). The exact molecular mechanism for how DEPs increase vascular permeability is not known, but one potential cause may be events initiated by direct contact of DEPs with alveolar endothelial cells. A small percentage of inhaled particles have been shown to reach the lung and gain access to the circulation, ending up in several compartments of the body (Brown et al., 2002; Geiser et al., 2005; Kreyling et al.,

Abbreviations: DEPs, diesel exhaust particles; HUVECs, human umbilical vein endothelial cells; PM_{2.5}, particulate matter with diameters equal to, or less than 2.5 μm; VE-cadherin, vascular endothelial cell cadherin.

* Corresponding author at: EOHSI and Department of Pharmacology and Toxicology, Ernest Mario School of Pharmacy, Rutgers University, 170 Frelinghuysen Rd, Piscataway, NJ 08854, United States. Tel.: +1 732 445 3751; fax: +1 732 445 0119.

E-mail address: magordon@eohsi.rutgers.edu (M.K. Gordon).

2002, 2009; Nemmar et al., 2001, 2002a; Oberdorster et al., 2004; Semmler et al., 2004; Shimada et al., 2006; Takenaka et al., 2006). Importantly, translocated particles may directly contribute to the increases in thrombotic activity that are observed in hamsters and humans after DEP exposure (Nemmar et al., 2002b, 2003), explaining some of the observed short-term adverse cardiovascular events.

Inflammatory mediators produced by many cell types likely contribute to the alveolar capillary leakage that results from DEP inhalation, and this complicates the identification of DEP-induced factors from individual cell types. We hypothesize that one of the effects of DEPs is a direct contribution to vascular permeability via disruption of endothelial cell–cell junctions. Barrier function is controlled by both the tight junctions (for review see Spring, 1998) and the adherens junctions (Corada et al., 2001), with adherens junctions controlling tight junctions via vascular endothelial (VE)-cadherin (Taddei et al., 2008). VE-cadherin is an endothelial specific cadherin of adherens junctions that regulates not only vascular permeability, but also leukocyte transmigration (Corada et al., 1999, 2001; Gotsch et al., 1997). To eliminate the contribution of the inflammatory cell response on vascular cell–cell junctions, and thereby examine the direct effect DEPs have on capillary structures, an *in vitro* culture system of pre-formed endothelial tubes was employed. The primary objective of this study was to use VE-cadherin as a marker of cell junction integrity in a system structurally related to capillaries, examining whether disruption of these molecules is one potential mechanism for how short-term (24 h) DEP exposures might induce an increase in vascular permeability in the lung.

2. Materials and methods

2.1. Diesel exhaust particles (DEPs)

Diesel exhaust particles (DEPs) were collected from a Japanese automobile engine by Dr. Masaru Sagai, who subsequently provided them to researchers at UCLA. Our group obtained them as a gift from Dr. David Diaz-Sanchez, formerly of UCLA. The particles have been characterized and used extensively (Bai et al., 2001; Inoue et al., 2006; Ito et al., 2000; Kumagai et al., 1997; Sagai et al., 1993; Singh et al., 2004). DEP powder (0.1 g) was suspended in 10 ml in PBS, 0.05% Tween-80 to make a 10 mg/ml DEP stock solution. Particles were then dispersed to achieve a particle size of PM_{2.5} (2.5 µm diameter and smaller) by vortexing for 3 min, then sonicating at 60 Hz for 5 min. To determine the range of sizes, an aliquot was fixed with 4% paraformaldehyde for examination at 630× magnification (Leica TCS SP2 Spectral Confocal Microscope). A more accurate assessment was made by dynamic light scattering using a Zetasizer Nano ZS90 with Malvern DTS software version 5.10 (Malvern Instruments, Malvern, MA). With this technique, particles are placed in a laser beam. The intensity of the scattered light fluctuates at a rate that is dependent upon the size of the particles, with smaller particles moving more rapidly. Analysis of the intensity fluctuations yields the velocity of the particles' Brownian motion. The particle size is then determined using the Stokes–Einstein equation for diffusion of spherical particles through liquid. Specifications were: temperature, 25 °C; material refractive index, 1.59; material absorption, 0.01; dispersant refractive index, 1.33; viscosity, 0.8881 centipoise; measurement position, 4.65 (mm). Six runs (120 s/run) were performed to determine mean particle diameter. For cell exposures, dilutions of the stock suspension to 1, 10 or 100 µg/ml in medium were made immediately after vortexing and sonicating. Additional concentrations of 5 and 50 µg/ml DEPs were prepared prior to modified LDH assays.

2.2. Endothelial cell culture

Medium used was EBM-2 Bulletkit medium (Lonza), an endothelial cell growth medium which contains 2% FBS, VEGF, hFGF-B, R3-IGF-1, ascorbic acid, heparin, and GA-1000 as purchased. In addition, since the DEPs were dissolved in 1× PBS (137 mM NaCl, 2.7 mM KCl, 10 mM sodium phosphate dibasic, 2 mM potassium phosphate monobasic, pH 7.4), 0.05% Tween-80, the medium was also supplemented to the same concentration with phosphate buffered saline and Tween-80, thereby minimizing differences between non-DEP-exposed controls and DEP-treated samples. In all cases below, the term “medium” refers to medium plus PBS–Tween-80.

Normal human umbilical vein endothelial cells (HUVECs) were obtained from Clonetics (Lonza Walkersville, Inc.) and used at passages 5–15. Cells were always plated at a density of 156 cells per mm². This translates to 6 × 10⁴ cells per well on the 12 well plates and 1.5 × 10⁵ cells per well on the 6 well plates. Cultures were incubated in a 5% CO₂ atmosphere at 37 °C in a volume of medium proportional

for the cell number, to insure that culturing parameters were always comparable between different well sizes. Medium was changed every day.

For monolayer cultures, HUVECs were plated on plastic tissue culture dishes. When used for assembling tube structures, cells were plated on the basement membrane substratum, Matrigel, a liquid at 4 °C which becomes solid at room temperature or above. LDEV-free Matrigel (BD Biosciences) at 10 mg/ml, 4 °C, was added to plates to completely coat the bottoms of 12-well (3.8 cm²/well) or 6-well (9.6 cm²/well) culture dishes residing on ice. Matrigel-coated dishes were transferred to the incubator to allow the substratum to solidify at 37 °C for 30 min before adding cells.

2.3. Preliminary assessments of endothelial tubes

Tube formation time was determined by seeding HUVECs onto Matrigel-coated dishes, and incubating them at 37 °C for 1, 2, 4, 6, 12 and 24 h. Cells were fixed with 4% paraformaldehyde for 10 min at room temperature. DAPI (1 ml/well of 300 nM final concentration in PBS) was used to stain nuclei in the samples after fixing. Phase contrast microscopy (Zeiss-Axiovert 40 Inverted Microscope) evaluated tube formation, and showed that by 12 h tube formation was totally complete, i.e., every DAPI stained nucleus resided in a cell participating in a tubular structure. For DEP exposure experiments, endothelial cells were plated on plastic (to form monolayers) or on Matrigel (to form tubes) at a density of 156 cells/mm² for 12 h, allowing the Matrigel samples to complete tube network formation. This 12 h post-plating time was defined as the “zero” time point in experiments. Endothelial tubes were incubated with either 0 µg/ml DEP (i.e., no DEP), or 1, 10 or 100 µg/ml dispersed DEPs in medium, unless otherwise indicated. Cultures were incubated at 37 °C for 24 h after the zero time point unless otherwise indicated.

Endothelial cell behavior as monolayers and as tube network cultures was compared. Proliferation was measured using the MTS assay, measuring mitochondrial enzyme activity via conversion of MTS (3-(4,5-dimethylthiazol-2-yl)-5-(3-carboxymethoxyphenyl)-2-(4-sulfophenyl)-2H-tetrazolium) and phenazine methosulfate to formazan (MTS kit, Promega). Three plates of cells were assayed at the zero time point (12 h after plating for both monolayers and endothelial tubes), another set of 3 at the 24 h post-zero time point, and a third set at 48 h post-zero time point. Cells were rinsed 3 times with cold PBS, then a mixture of 60 µl water-soluble kit reagent plus 300 µl fresh medium was added to each well for a 1 h incubation at 37 °C in the dark. Supernatants (100 µl/well) were collected and the absorbance of the generated formazan was measured at 490 nm. This absorbance reflects the total number of cells in each sample, and allows calculation of doubling time.

2.4. Modified LDH cytotoxicity assay to detect cell survival after DEP exposure

DEP cytotoxicity to endothelial tubes was evaluated using the CytoTox-Homogeneous Integrity Assay Kit (Promega), a method that measures cytosolic lactate dehydrogenase (LDH) released into medium when cells are lysed. The method was adapted to remove particles and dead cell-derived-LDH from the living cells after DEP exposure, to ensure the DEPs would minimally interfere with the assay. Plates of formed endothelial tubes were exposed to medium alone (the no DEPs control) or medium containing DEPs (1, 5, 10, 50, and 100 µg/ml medium) for a 24 h 37 °C incubation. Next, medium (containing LDH from dead cells and floating cell debris) was aspirated from the cultures. Endothelial tube cells were then washed 3 times in cold PBS. Cells were collected by centrifugation and lysed for 1 h in 200 µl lysis solution (Promega) following the manufacturer's instructions. The relative fluorescence (described in RFUs, relative fluorescence units) of LDH was measured at 490 nm. Unexposed cultures were used as the positive control, defining the maximum amount of LDH potentially released. This value was defined as 100%. With the adaptation described, the absorbance levels of DEP-exposed samples represent cells surviving the exposure, and were expressed as a percentage of the control unexposed sample.

2.5. VE-cadherin immunofluorescence

HUVECs (6 × 10⁴ cells/well, plated at 156 cell/mm² density) were seeded onto Matrigel-coated 2-well chamber slides for tube formation prior to DEP exposures for 24 h. After exposure, endothelial tubes were rinsed with PBS and fixed with 4% paraformaldehyde for 10 min at room temperature. Nonspecific reactivity of HUVECs was blocked by addition of 2% normal goat serum with 0.02% sodium azide (NaN₃) in PBS for 1 h at room temperature. The endothelial tube cells were then incubated with primary anti-human VE-cadherin (BD Biosciences) monoclonal antibody at a 1:50 dilution (20 µl in 1 ml blocking buffer, i.e., 2% normal goat serum) for 1 h at room temperature. Goat anti-mouse secondary antibody labeled with Alexa 488 (green color, Jackson Immuno Research) was used at a 1:100 dilution (10 µl in 1 ml PBS) for 1 h at room temperature. When wide field (epifluorescence) microscopy was used, nuclei were stained by incubating endothelial tubes in 300 nM DAPI for 5 min at room temp, followed by washing with PBS/Tween for 5 min. When confocal microscopy was used, nuclei were stained by adding 1 ml 20 µM DRAQ5 (Alexis) for 10 min at room temperature to each well. Slides were covered with Prolong Gold (Invitrogen) anti-fade mounting media and incubated at 4 °C overnight. All images were observed at 100× and 400× magnifications on an epifluorescence microscope

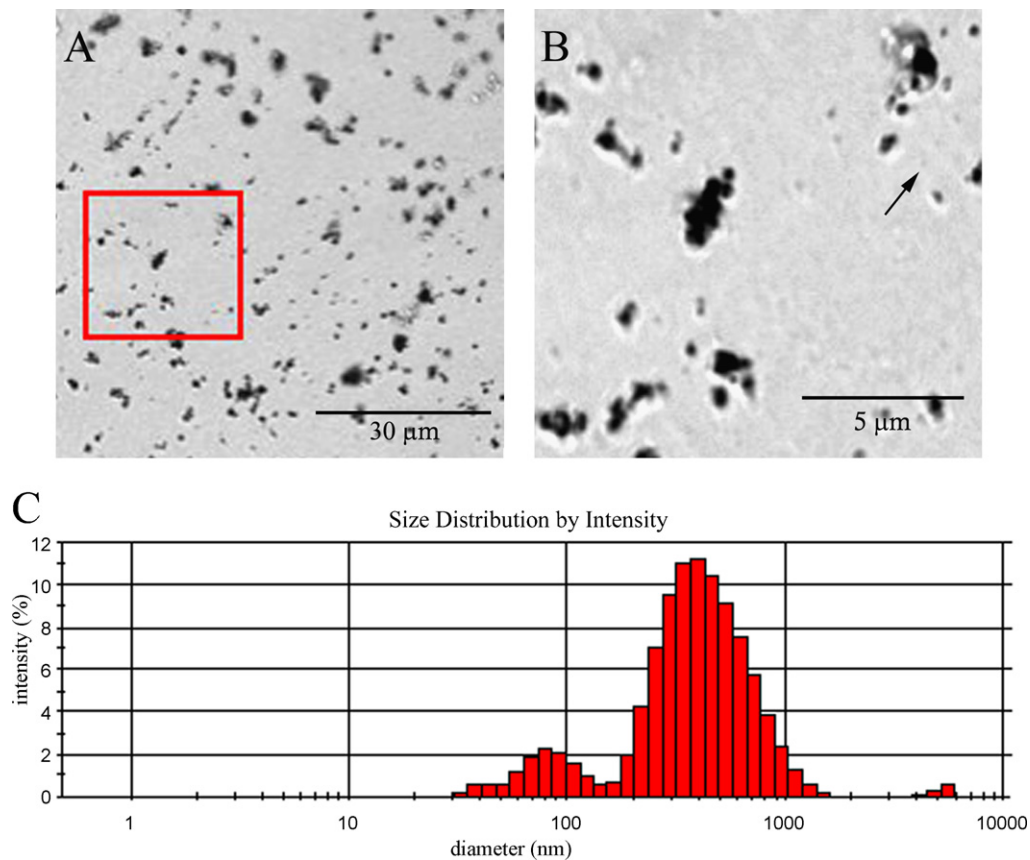


Fig. 1. Light microscopy and dynamic light scattering of DEPs. Phase contrast images obtained on the Leica TCS SP2 Spectral Confocal Microscope to determine the distribution of particle shapes, sizes and diameters, taken at 630 \times magnification with magnification bars. Panel A, DEPs diluted in PBS containing 0.05% Tween-80, then vortexed 3 min, followed by sonication for 5 min. The majority of particles are PM_{2.5}; panel B, enlarged image of the area enclosed by the red square in panel A. Many particles are of very small sizes. Several have diameters of 0.1 μ m (PM_{0.1}), the limit of light microscopy. The arrow points to a particle of this size. Panel C, size distribution of particles by dynamic light scattering using a Zetasizer Nano ZS90 shows that the mean of 6 runs (120 s/run) revealed the average particle diameter was 254.7 nm \pm 138.7 SD; 85% of these particles had a mean diameter of 380 nm; 14% were in the ultrafine range (PM_{0.1}, equal or less than 0.1 μ m, i.e., 100 nm), averaging 80 nm in diameter. (For interpretation of the references to color in this figure legend, the reader is referred to the web version of the article.)

(Olympus IX71 Inverted Microscope) or at 630 \times magnification (water lens, N.A. 1.3) on a Leica TCS SP2 Spectral Confocal Microscope.

To evaluate the extent of the VE-cadherin disruptions in the plasma membrane induced by DEP exposure, confocal images of a random selection of cells in endothelial tube networks were examined where 30 μ m or more of plasma membrane was found in the plane of focus. Magnification of these 30 μ m stretches of plasma membrane showed that interruptions of \sim 4 μ m were not uncommon in unexposed endothelial tube cells, therefore these were considered to represent regions where the cell membrane moved out of the plane of focus. However, 3 μ m interruptions in the fluorescent pattern were increasingly predominant after exposure to increasing concentrations of DEP, therefore they appeared to represent DEP-induced disruptions in VE-cadherin, and were tallied. This size criterion was defined to unbiased the hand counting of interruptions as much as possible, and yields an analysis that represents a trend, and is referred to as a semi-quantitation. About 200 cells from 12 different control samples, as well as 12 different samples of each exposure condition, were examined. The endothelial membranes of the 100 μ g/ml DEP-exposed samples were too disrupted to assess for discontinuities. Internalized globules of VE-cadherin were also assessed: Areas where immunofluorescent VE-cadherin pulled away from the membrane toward an intracellular position were counted. Globules were scored as equal to or under 10 μ m or greater than 10 μ m, and were assessed in \sim 200 cells from each set of samples.

2.6. Western analyses

After 24 h DEP exposure, the endothelial tube cells were collected with the Matrigel at room temperature and sonicated for 1 min in lysis buffer (20 mM Tris-HCl, 0.5% deoxycholate, 0.5% SDS, 1% Triton X-100, 1% Nonidet P-40, 1 mM Na₃VO₄ and 0.1% protease inhibitor). The solid Matrigel and cell debris was removed by centrifugation at 10,000 rpm for 10 min at room temperature. The protein concentration of the supernatant was measured by absorbance at 540 nm using the bicinchoninic acid method (BCA Protein Assay, Pierce). Twenty micrograms/well were loaded onto SDS polyacrylamide gels for electrophoresis. Proteins were

transferred to 0.45 μ m PVDF membrane using electrophoretic transfer (Bio-Rad). Nonspecific reactivity was blocked for 1 h at room temperature with standard 1 \times TBST buffer containing 3% BSA and 0.02% NaN₃. Primary antibody against VE-cadherin (BD Biosciences), diluted 1 to 1000, or against β -catenin (Abcam), diluted 1–2000, or against actin (Sigma), diluted 1–1000, or against glyceraldehyde-3-phosphate dehydrogenase (GAPDH, Sigma), diluted 1–5000 with blocking buffer, was added to a blot and incubated overnight at 4 $^{\circ}$ C. After washing in 1 \times TBST, secondary antibodies conjugated with horseradish peroxidase (HRP) were diluted 1–5000 in 5% milk, 1 \times TBST, and applied to the blots for a 1 h incubation at room temperature. Blots were then reacted with ECL reagent (Pierce) containing luminol, a substrate of horse radish peroxidase (HRP), and exposed to X-ray film.

2.7. Statistics

For HUVEC proliferation, the data included 3 replicates from a single experiment. Thus, a one-way analysis of variance (ANOVA) was used to examine differences in time with Dunnett's procedure to compare 6, 24 and 48 h to baseline (0 h).

For the LDH values at 24 h, a mixed model analysis evaluated the differences between DEP concentrations of 0, 1, 5, 10, 50 and 100 μ g/ml. Three experiments were conducted on different days with three replicates at each concentration for each experiment. The average relative fluorescent unit per dose, with the background average subtracted off, was used as the unit of experiment. As such, analysis was conducted using a mixed model with dose as a fixed effect and a random effect for experiment/day. Dunnett's procedure, creating *p*-values that are adjusted for multiple testing, was used to compare all non-zero doses to the zero exposure.

For discontinuities and globules, binomial regression was used to compare the probability of discontinuity/globularity for each nucleus (i.e., per cell). In this approach, the number of cells on the slide per nucleus is considered as the number of trials with the number of discontinuities/globules out of that number modeled as a binomial response variable, with dose (0, 1, or 10 μ g/ml of DEP) predicting the probability of discontinuity or globularity within each cell. A Wald Chi-square test was used to evaluate the effect of dose, with a Bonferroni correction applied (indi-

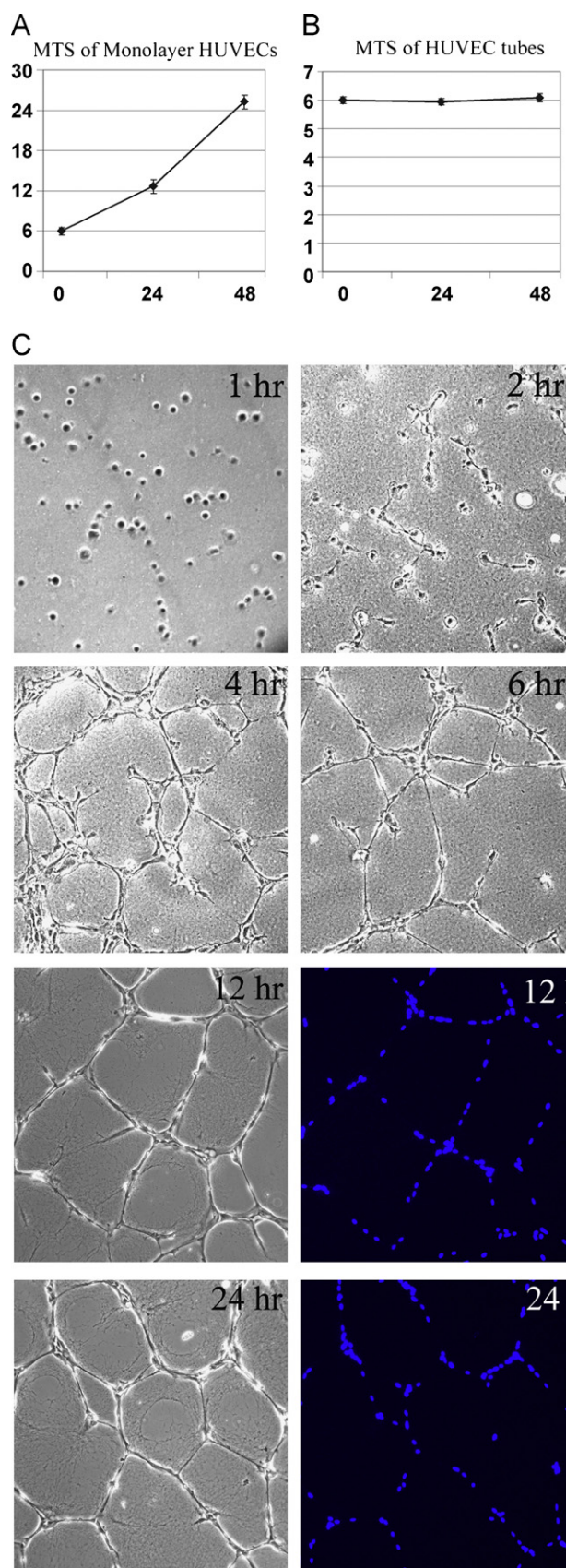


Fig. 2. Characteristics of HUVEC endothelial tubes. (A) Monolayers of HUVECs doubled every 24 h. The effect of hours post-baseline was significant ($F=340.23$, $d.f.=3,8$, $p<0.0001$). Proliferation at 24 and 48 h differed significantly from baseline ($t=9.67$ and 27.86 , with $d.f.=8$ and adjusted $p<0.0001$ for both). (B) Pre-assembled HUVEC tubes did not show proliferation at any of the time points as evidenced by the

Table 1
Cytotoxicity of DEP on HUVEC tubes.

Conc. of DEP ($\mu\text{g/ml}$)	LDH at 24 h Cell survivability (%)
0	100 ± 0.36
1	90.4 ± 1.87
5	$84.0 \pm 0.79^*$
10	$80.7 \pm 4.31^*$
50	$60.2 \pm 0.77^*$
100	$49.6 \pm 8.25^*$

Cell Survivability of HUVECs in tube cultures treated with DEP for 24 h, as assessed by modified LDH assays. Because LDH liberated from killed cells had been removed along with the DEP in the medium and washes, lysis of the remaining cells generated LDH values representative of surviving cells. The unexposed sample absorbance was set at 100% survival. The ratio of exposed absorbance to unexposed yielded the % of cells surviving each exposure condition. Data are expressed as the mean \pm SD of three independent experiments, each performed in triplicate (i.e., 9 plates).

* $p<0.05$ to the cell control ($0 \mu\text{g/ml}$).

vidual significance level of 0.025 applied to each comparison in order to maintain a family-wise error rate of 0.05) when comparing each non-zero dose to the zero dose. A value of $p<0.05$ was considered statistically significant. Statistical inference was not appropriate for the $100 \mu\text{g/ml}$ DEP-exposed samples. Observations have been described as best as possible, but statistical significance cannot be calculated.

3. Results

3.1. Diesel exhaust particles (DEPs) and endothelial cells

We hypothesized that, by exposing *in vitro* endothelial tubes in culture to DEPs, the direct effects of particles on *in vivo* capillaries might be revealed, suggesting possible mechanistic information about how DEPs affect capillary endothelia *in vivo*. The DEPs employed were dispersed to typical respirable sizes, $\text{PM}_{2.5}$, as assessed by light microscopy and Zetasizer Nano ZS90 dynamic light scattering (Fig. 1). About 14% of the DEPs fit the size designation of $\text{PM}_{0.1}$ (100 nm diameters or smaller, a.k.a. nanoparticles and ultrafine particles), and appear as the bars between 30 and 100 nm in the Fig. 1 histogram.

Human umbilical vein endothelial cells (HUVECs) have proven useful for particulate exposure studies (Garcia et al., 1989; Sumanasekera et al., 2007; Waldman et al., 2007; Yamawaki and Iwai, 2006) and therefore were chosen for this study. However, the goal was to use them in a tubular capillary-like network structure that would retain characteristics of the *in vivo* vasculature, and this can be accomplished by plating them on the basement membrane substratum, Matrigel. Unlike HUVECs in monolayer culture, which doubled every 24 h as determined by the MTS assay (Fig. 2A), HUVEC tubes displayed the *in vivo* capillary endothelia property of prohibited proliferation (Fig. 2B). All HUVECs plated on Matrigel were involved in tubular networks by 12 h (Fig. 2C), thus, DEP were added to experimental cultures at this time.

3.2. DEP-induced endothelial tube cell death is concentration dependent

An adapted cytotoxicity assay was used that first removed LDH released by cells killed during the incubation with DEPs, prior to liberating LDH from cells surviving the DEP exposure. By compar-

absorbance remaining unchanged at all time points. Despite the many unoccupied regions on the plate, endothelial tubes maintained the *in vivo* capillary endothelial characteristic of being strictly prohibited from uninduced proliferation. (C) The timing for tube formation was assessed and determined that by 6 h tube formation was mostly complete, and by 12 h it was totally complete. Comparing phase contrast images with DAPI stained nuclear images at 12 and 24 h demonstrated that no nuclear stain was evident in any area on the plate that was not part of a tube structure, indicating that every cell was incorporated into the tubular network. This is true for both the 12 h and the 24 h time points (magnification $100\times$).

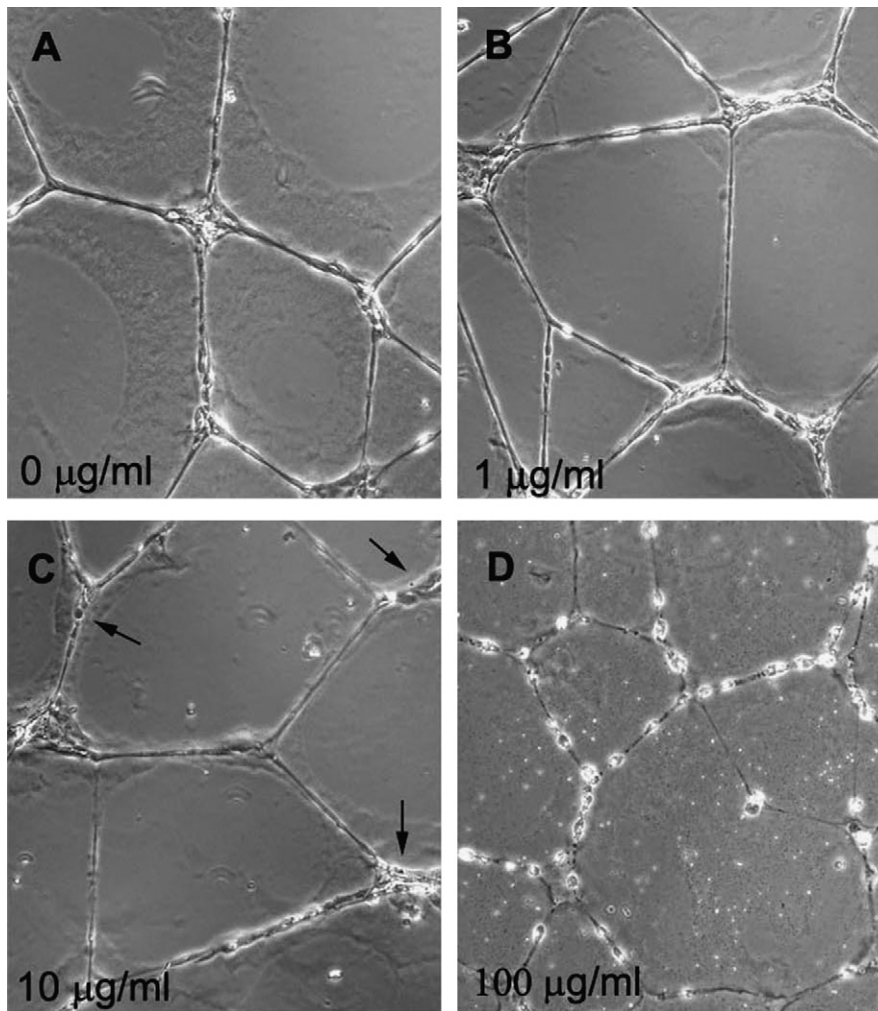


Fig. 3. Phase contrast micrographs of endothelial capillary-like tubes exposed to various concentrations of DEPs for 24 h. Panel A, unexposed control; panel B, medium containing a final concentration of 1 µg/ml DEPs; panel C, medium containing a final concentration of 10 µg/ml DEPs; panel D, medium containing a final concentration of 100 µg/ml DEPs. Arrows in panel C point to individual diesel particles apparently associated with the tube network cells, magnification 100×.

ing the LDH relative fluorescence unit (RFU) value of all samples at 24 h, and using the unexposed control LDH RFU value as the 100% live cell value, the percentage of cells surviving DEP exposure was calculated. The data demonstrate that increasing concentrations of DEPs reduced the level of cell survival (Table 1). Ninety percent of the plated cells survived a 24 h exposure to 1 µg/ml DEPs. At 5 µg/ml, 10 µg/ml, and 50 µg/ml DEPs, the 24 h cell survival was 84%, 81%, and 60%, respectively. Only ~50% survived exposure to 100 µg/ml DEPs. Although DEP toxicity is apparent from the LDH assays, tubes retained the skeleton of their tube network structure (Fig. 3), even with the highest DEP concentration. A phase contrast image of a 100 µg/ml DEP exposure sample shows that about half of the endothelial tube cells are elongated, similar to cells not exposed to DEPs, and about half of the cells are rounded up (Fig. 3D), suggesting a loss of cell–cell contact.

3.3. DEP exposure causes redistribution of VE-cadherin

To investigate whether DEP exposure directly affects cell–cell contacts within the adherens junctions, vascular endothelial cell cadherin (VE-cadherin, a.k.a. cadherin-5) was examined. To investigate the cell–cell junctional integrity of endothelial tubes after DEP exposure, epifluorescence of 3 separate DEP exposure experiments was performed using antibody against VE-cadherin. As seen in Fig. 4A–C, VE-cadherin is at the cell borders of non-exposed cul-

tures, outlining the cells in a regular pattern. After a 24 h exposure of endothelial tubes to 1 µg/ml of DEPs, the pattern of VE-cadherin is similar to the unexposed control tubes (Fig. 4D–F), but with a few local accumulations of staining (arrows in Fig. 4 panels E and F). The 10 µg/ml DEP samples show an increase in changes in the distribution of VE-cadherin (Fig. 4G–I, see arrows). While much of the VE-cadherin is found sharply localized to the plasma membrane, variable sized spherical cytoplasmic globules of VE-cadherin were sporadically observed, and were frequently associated with a loss of sharpness at the cell–cell junction at the plasma membrane. This indicated loosening of the VE-cadherin from the membrane and a relocalization of the molecule into the intracellular space. At the 100 µg/ml concentration of DEPs (Fig. 4 panels J–L) the VE-cadherin is highly internalized, with very little remaining at the cell–cell junctional area.

Because of their three-dimensional structure, endothelial tubes are not typical cultured cells, and small local changes in cell junctions are masked in wide field epifluorescence, since it is a summation of all the planes of a 3D image. To better evaluate VE-cadherin redistribution after exposure to the lowest DEP concentration, 1 µg/ml, single optical planes were viewed by confocal microscopy. In the unexposed controls used for comparison (Fig. 5A–C), VE-cadherin outlined the endothelial cell membranes where they are in the plane of focus. Many cells showed only a portion of the membrane in this plane. Occasionally a small dis-

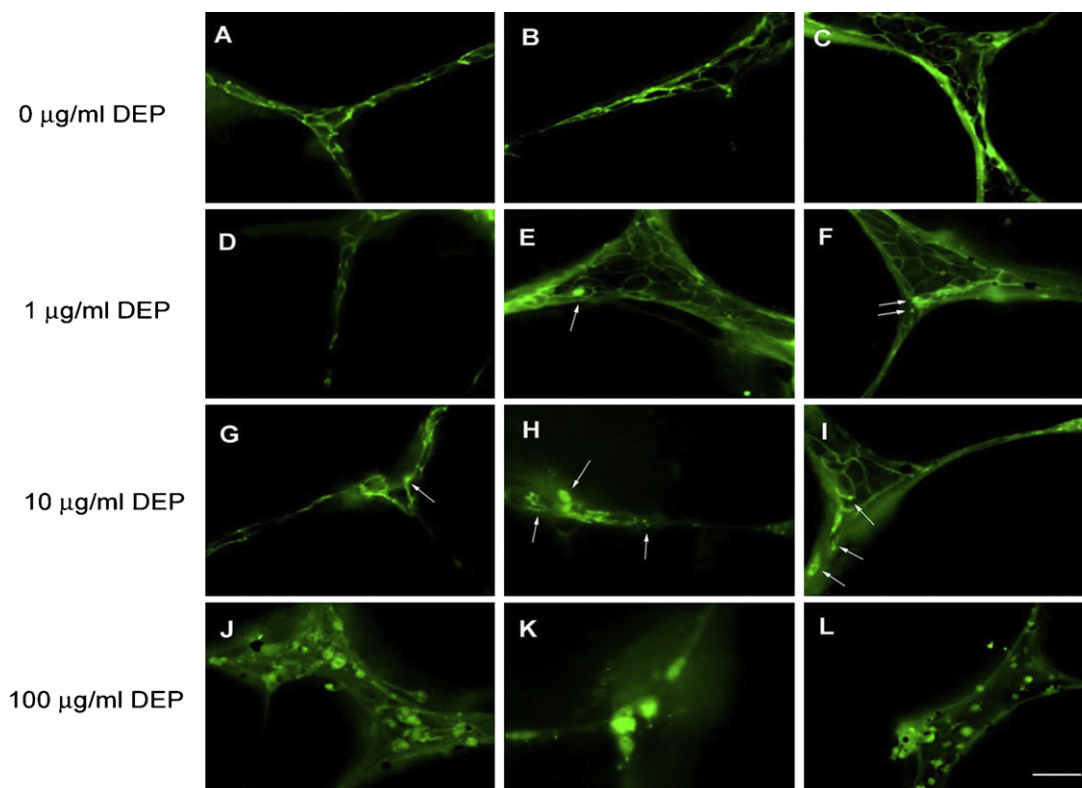


Fig. 4. Widefield epifluorescence microscopic immunolocalization of VE-cadherin in endothelial tubes treated with DEPs for 24 h. Panels A–C, control, 3 cultures of unexposed endothelial tubes; panels D–F, endothelial tubes exposed to 1 $\mu\text{g/ml}$ DEPs; panels G–I, 3 cultures of endothelial tubes exposed to 10 $\mu\text{g/ml}$ DEPs; panels J–L, endothelial tubes exposed to 100 $\mu\text{g/ml}$ DEPs. Arrows indicate globular accumulations of VE-cadherin antibody staining. The images were obtained on an Olympus IX71 Inverted Microscope at 400 \times magnification. All images were obtained with the same digital camera settings. Scale bar = 30 μm .

continuity of less than 3 μm (arrowhead in panel A), or a globule (arrow in panel A) was observed. With 1 $\mu\text{g/ml}$ DEP exposures, confocal microscopy did, indeed, demonstrate that the number of VE-cadherin discontinuities (Fig. 5D–F arrowheads) and globules (Fig. 5D–F arrows) were more frequently observed than in unexposed samples. At 10 $\mu\text{g/ml}$ DEPs (Fig. 5G–I) many more punctate spots of VE-cadherin are observed, indicating local alterations to the adherens junctions. At 100 $\mu\text{g/ml}$ DEPs (Fig. 5J–L) the VE-cadherin is extensively intracellular, suggesting extensive dissolution of the adherens junctions, as seen with epifluorescence.

A semi-quantitation of the changes in VE-cadherin was derived from the confocal images. Discontinuities in the plasma membrane of 3 μm or less were counted for the 0, 1 and 10 $\mu\text{g/ml}$ DEP samples, as indicated in Fig. 6A. About 200 cells from 12 different samples were assessed. Some apparent discontinuities of VE-cadherin staining should represent the natural positioning of the plasma membrane in and out of the plane of focus. Others should represent local breaks in adherens junctions in the membrane. Close examination revealed that discontinuities of 4 μm or larger were relatively constant at all DEP concentrations, making it likely they were membrane out of the plane of focus, while the number of small discontinuities (\sim 3 μm or smaller, arrows in Fig. 6A) rose with increasing DEP concentration. These small discontinuities were scored as likely direct effects of DEP on VE-cadherin and are represented in Fig. 6B. A second assessment was of the number and size range of fluorescent globules of internalized VE-cadherin, as indicated in Fig. 6C. Globules of 10 μm or less were tallied (arrows, Fig. 6C), as were those greater than 10 μm . Smaller globules increased in number with increasing exposure concentrations, and are the predominant size in 1 and 10 $\mu\text{g/ml}$ DEP exposures. However, with 100 $\mu\text{g/ml}$ DEP exposures, globules were pervasive, with the $>10 \mu\text{m}$ being more abundant than the

smaller ones (Fig. 6D). These data demonstrate that increasing concentrations of DEPs lead to an increasing trend for VE-cadherin to leave the plasma membrane (as shown by discontinuities), and to become aggregated intracellularly (as shown by globules).

The fact that the intensity of the VE-cadherin fluorescent signal merely reallocated, but did not seem to diminish with increasing DEP concentration, was of interest. To examine this further, unexposed and DEP-exposed tubes were collected and lysed for protein extraction. Western analyses showed that the levels of VE-cadherin, as well as β -catenin, were not significantly altered with increasing DEP concentration (Fig. 7). VE-cadherin appeared as a 130 kD band, present in the unexposed control endothelial tube extracts, as well as the DEP-exposed extracts. Thus DEPs had a minimal effect on the total amount of VE-cadherin. The change in VE-cadherin was primarily in its localization.

3.4. DEPs gain access to endothelial tube cells

Whether pre-formed *in vitro* endothelial tubes were capable of translocating particles, perhaps allowing them into the luminal space, was assessed by confocal microscopy. After a 24 h exposure, many images visualized DEPs in the vicinity of tubes. Fig. 8A shows several particles in a phase contrast image from a 10 $\mu\text{g/ml}$ DEP exposure. The cross-lines in Fig. 8B show where z stack images were captured from the confocal plane of focus. The image shows the z plane representing the mid-height of the three-dimensional structure, and shows 2 diesel particles (arrows) at the level of the nuclei. This indicates the particles are in the interior of the cells. In Fig. 9, a phase contrast image is overlapped with the confocal z plane images focused at the top of the tube (panel A), at the middle of the tube (panel B), and at the bottom of the tube, close to the Matrigel (panel C). The cross-hairs show a particle that is in sharp focus when

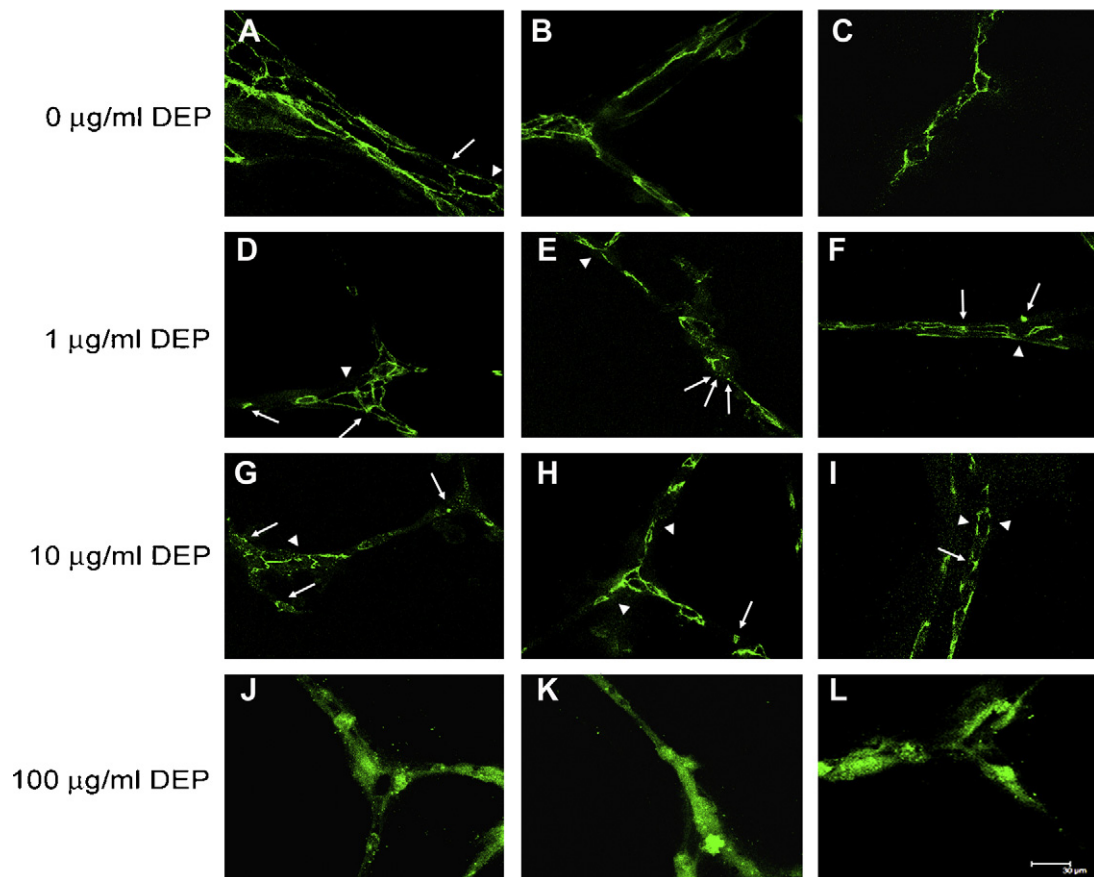


Fig. 5. Confocal images of single optical sections to detail the distribution of VE-cadherin in response to DEP exposure for 24 h. Panels A–C, unexposed control endothelial capillary-like tubes; panels D–F, endothelial tubes exposed to 1 µg/ml DEPs; panels G–I, tube networks exposed to 10 µg/ml DEPs; panels J–L, endothelial tube networks exposed to 100 µg/ml DEPs. Arrowheads show discontinuities in VE-cadherin staining and arrows show punctate globules of staining. In J–L, VE-cadherin staining was diffuse throughout the cell cytoplasm. Images were obtained using a Leica TCS SP2 Spectral Confocal Microscope at 630× magnification using identical settings for all photos. Scale bar = 30 µm.

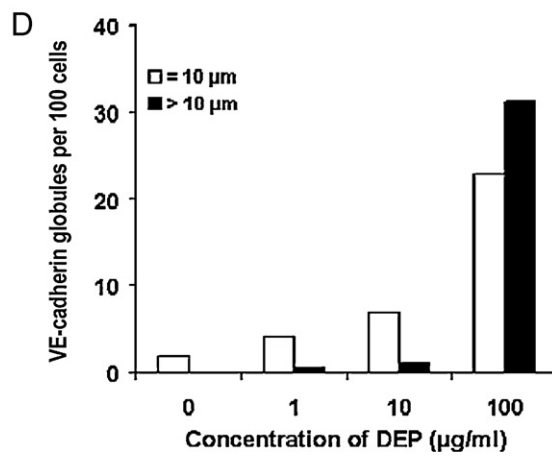
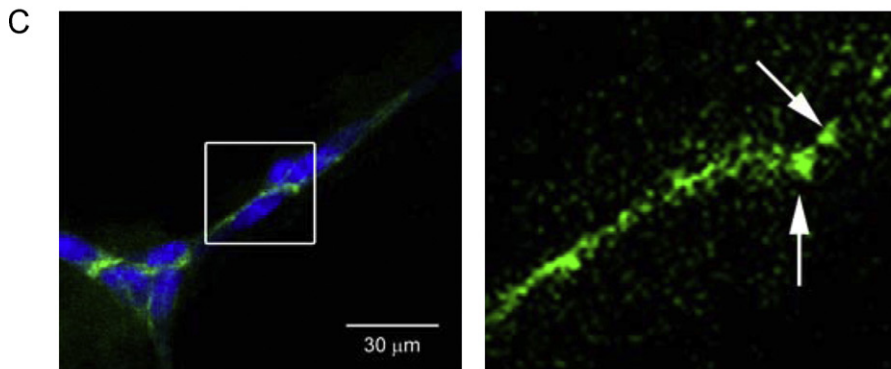
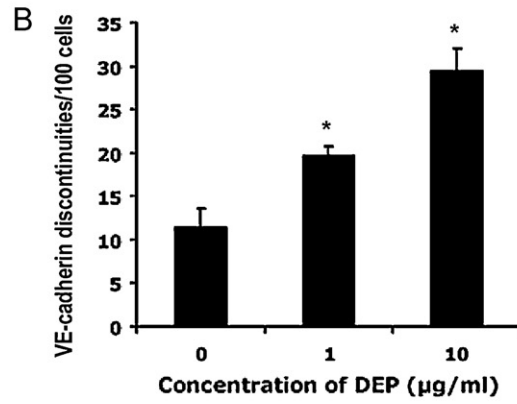
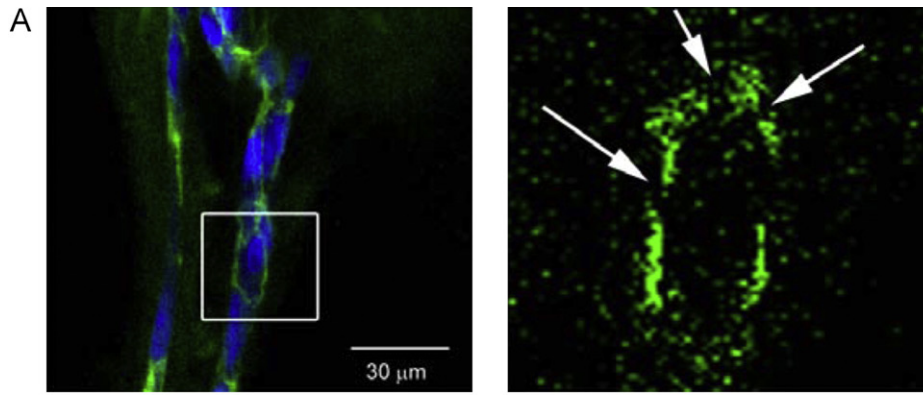
the z-section is focused on the middle of the structure. In addition, as seen in the bottom z plane bar image, the particle appears to be surrounded by the green fluorescence of the VE-cadherin. The side y and bottom z plane bar images together suggest that the particle is likely contained in a tube lumen (Fig. 9B). Since particles are added after tube networks are formed, the confocal images in Figs. 8 and 9 suggest that DEPs are translocated to sites either within the endothelial tube cells, or possibly within the tubular lumen.

4. Discussion

Our primary goal was to determine whether a 24 h exposure of an endothelial tube network to DEPs would show a direct effect on the endothelial cells. HUVECs were chosen as the endothelial cells for the experiments because of their previous use in studying the consequences of particulate exposures (Garcia et al., 1989; Sumanasekera et al., 2007; Waldman et al., 2007; Yamawaki and Iwai, 2006) and because of the hundreds of publications using their tube formation as the gold standard angiogenesis assay. Also, studies over the last 30 years have suggested that these *in vitro* formed tubes have many similarities with *in vivo* capillaries (Grant et al., 1991; Zimrin et al., 1995; Donovan et al., 2001). Not only does the morphology of endothelial tubes approximate that of *in vivo* capillaries, but once the endothelial cells are in tube networks, their proliferation is prohibited, as we show here (Fig. 2). Restricted proliferation is a hallmark of *in vivo* capillary endothelial cells (Hadley et al., 1985). Furthermore, electron microscopic analysis has demonstrated that capillary tubes formed *in vitro* and *in vivo*

endothelia have the same adherens junction structures (Schmelz and Franke, 1993; Zhou et al., 2004), which are crucial in controlling permeability (for review see Dejana et al., 2008). The DEPs used in the study are well characterized (Bai et al., 2001; Inoue et al., 2006; Ito et al., 2000; Kumagai et al., 1997; Sagai et al., 1993; Singh et al., 2004) and of biologically relevant sizes, being dispersed to PM_{2.5} (Fig. 1). Thus, the sizes used in the *in vitro* experiments are those of respirable particles (Oberdorster et al., 1994; Jaques and Kim, 2000; Kreyling et al., 2002, 2009; Nemmar et al., 2006), which might access the alveolar-capillary complex, a site where the capillary endothelium is covered by only a thin layer of alveolar type I cell membrane. In this region, particles may be able to directly encounter and affect endothelial cells.

In vivo, mice exposed to the same sample of DEPs as used here responded with lung inflammation and vascular leakage within 4 h. Inflammatory cells were also found in bronchoalveolar lavage fluid (Singh et al., 2004). *In vivo*, increases in vascular permeability could be either from a direct effect of DEPs on the endothelial cells, or could result as a consequence of neutrophil and macrophage activation and mobilization. Since disruption of the VE-cadherin-containing adherens junctions has been shown to cause vascular permeability and leakiness (Gallicano et al., 2001; Kevill et al., 2001; Venkiteswaran et al., 2002; Villasante et al., 2007; for review see Dejana et al., 2008), we assessed whether disruption of VE-cadherin occurred in endothelial tubes as a direct response to DEP exposure, and found that this was the case. Our data demonstrate that increasing concentrations of DEPs increasingly disrupted VE-cadherin (Figs. 4–6). Interestingly, the lowest concentration of DEPs



(1 $\mu\text{g/ml}$) caused only focal internalizations of VE-cadherin, and minimal cell death. It is expected that this would mimic the *in vivo* situation, since the vascular permeability caused by inhalation of DEP has never been reported to be coincident with alveolar endothelial cell death. Furthermore, the advantage of using *in vitro* endothelial capillary-like tubes is that the effect of DEPs was assessed in the absence of immune cells, and indicated that DEPs were able to directly affect endothelia, altering the location of VE-cadherin by internalizing it. Vascular permeability has been shown to increase when VE-cadherin is internalized (Xiao et al., 2005). Internalization did not alter the amount of VE-cadherin, nor its electrophoretic mobility. β -Catenin and actin also did not change in amount or mobility. Although the *in vitro* system used in these experiments is not a perfect model system for what occurs *in vivo*, the results reported here are not inconsistent with what is seen in DEP-induced lung vasculature permeability *in vivo* and suggest that DEPs reaching the lung vasculature may affect permeability by causing localized internalization of VE-cadherin. By what mechanism might this occur? Since DEPs cause oxidative stress (Baulig et al., 2003; Li et al., 2002; Nel et al., 1998; Riedl and Diaz-Sanchez, 2005; Sagai et al., 1993; Wan and Diaz-Sanchez, 2007), reactive oxygen species are factors that may induce vascular permeability (Bai et al., 2001; Lei et al., 2005; Matsunaga et al., 2009). This idea is attractive because endothelial monolayers treated with hydrogen peroxide internalize VE-cadherin and become more permeable (Kevil et al., 1998). Alternatively, DEPs may induce endothelial hypoxia, leading to release of vascular permeability factor/vascular endothelial cell growth factor (VPF/VEGF). The normal interaction of the VEGF receptor with VE-cadherin in the cell membrane makes adherens junctions a downstream target of VPF/VEGF (Esser et al., 1998; Kevil et al., 1998). Future work will investigate this.

Our secondary goal was to examine whether DEP could translocate into pre-formed capillary-like tubes. This is of interest because some evidence indicates that *in vivo* particles are engulfed by

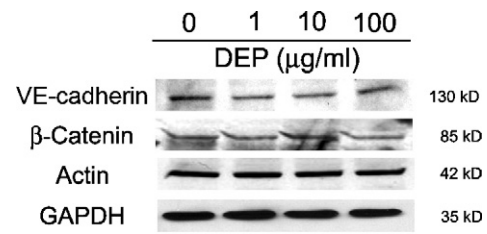


Fig. 7. Endothelial tubes exposed to 0, 1, 10 or 100 μg DEPs for 24 h were separated from the Matrigel, and used to extract protein for Western analysis. Antibodies against the adherens junction proteins VE-cadherin and β -catenin were used to probe the blots. Stripping the blots to reprobe with antibody against actin and glyceraldehyde-3-phosphate dehydrogenase assured that equal amounts of protein were loaded in the wells.

macrophages (Alexis et al., 2006; Geiser et al., 2005, 2008; Takenaka et al., 2006) and this might allow transport of particles to regions distal to the airways, such as into the circulation. Unequivocal evidence demonstrating translocation via a direct interaction between particles and *in vivo* endothelia is lacking, therefore, showing a direct interaction between endothelial tube networks and DEPs *in vitro* supports the idea that a particle encountering an alveolar endothelium might enter a cell and/or cross into the vessel lumen. In rats, inhalation of an ultrafine TiO_2 aerosol demonstrated that some particles were found in the microvasculature 1–24 h after exposure. Cellular uptake of particles was not by endocytosis, but rather by diffusion or adhesive interactions (Geiser et al., 2005). Using confocal microscopy, we show *in vitro* both entry of particles into the cytoplasm of endothelial cells in tube structures, and entry into the luminal space of the endothelial tube (Figs. 8 and 9). Although the mechanisms by which particles were translocated is not known, the data are not inconsistent with the idea that DEPs can gain access to the *in vivo* vasculature, where they might interact with platelets or initiate an immune response, or where they might

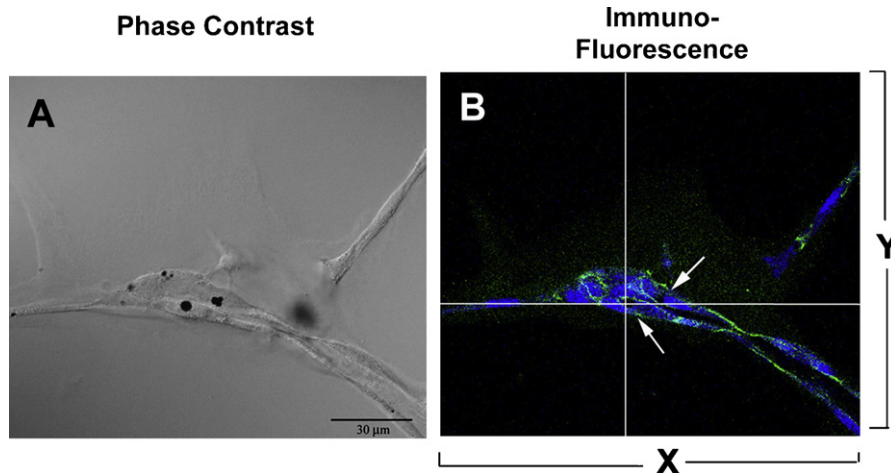


Fig. 8. A phase contrast image (panel A) and a z plane confocal image (panel B), taken midway through the depth of a HUVEC tube, is focused at the point where the x and y plane lines intersect. Green color indicates VE-cadherin antibody staining, and blue is nuclear staining with DRAQ5. Two diesel particles (arrows) are at the same depth in the tube structure as the blue stained nuclei (panel B). Scale bars = 30 μm .

Fig. 6. Semi-quantitation of VE-cadherin discontinuities and globules. In panel A, left side, the boxed region shows an example of $\sim 33 \mu\text{m}$ of endothelial tube plasma membrane in the plane of focus. This box was magnified and is shown on the right side of the panel. The blue DRAQ5 nuclear stain overlay was removed, and the number of interruptions in the green VE-cadherin fluorescence pattern, representing discontinuities 3 μm or less in length, were counted (arrows). The large discontinuity on the right side of the tube (without an arrow) is 4.7–5 μm , and was considered membrane going out of the plane of focus, rather than being an alteration of VE-cadherin in the membrane. This larger size disruption is relatively common in single confocal planes in the unexposed tube networks. Panel B is a compilation of the discontinuities found in about 12 different samples of each DEP concentration (0, 1, and 10 $\mu\text{g/ml}$). For unexposed samples, 215 cells were assessed; for 1 $\mu\text{g/ml}$ samples, 192 cells; and for 10 $\mu\text{g/ml}$ samples, 202 cells were examined. The VE-cadherin pattern of the 100 $\mu\text{g/ml}$ DEP exposed samples is not shown, since the fluorescence was mostly all intracellular. Panel C, left, contains an example of an area where VE-cadherin in the plane of focus formed globules. This area was magnified and is shown as the right side of the panel. Arrows indicate 2 fluorescent VE-cadherin globules, one $\sim 2.4 \mu\text{m}$, and the other $\sim 1.6 \mu\text{m}$. Globules such as these were counted and scored as either equal to or under 10 μm , or as greater than 10 μm . Panel D shows histograms compiling the number of globules in ~ 200 cells from 12 different samples from each DEP concentration. Globules represent VE-cadherin pulling away from the membrane, disrupting adherens junctions.

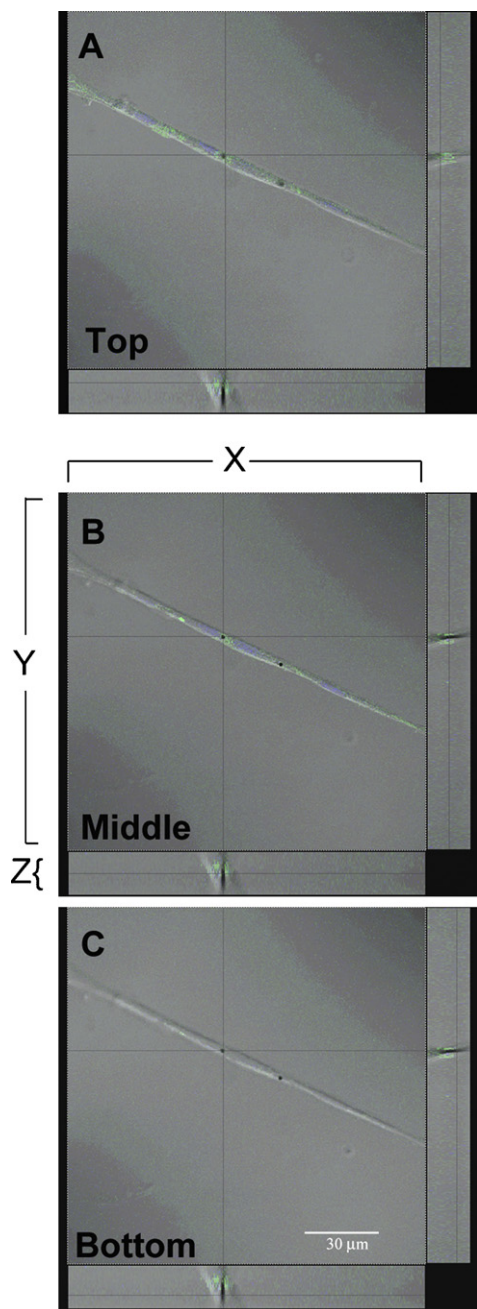


Fig. 9. Overlaid phase contrast (gray colored transmitted image) with confocal images of an unbranched endothelial tube containing two visible diesel particles. VE-cadherin is detected with green labeled secondary antibody. The x and y axis lines intersect at the point where the microscope was focused for the z stack analysis. In the fluorescent images, the z plane was focused at the top of the endothelial tube (panel A), at the middle of the tube (panel B), and at the bottom of the endothelial tube (panel C). The appearance of the particle in these planes demonstrates it is not on the exterior of the HUVEC tube, nor is it under the tube structure in the Matrigel. Rather, it is internal in the endothelial tube structure, as evidenced by the sharpness of the particle's appearance in the middle panel, and by the z plane bar images at the bottom of each panel. Scale bar = 30 µm.

induce thrombus formation, as has been demonstrated (Lucking et al., 2008). If translocated DEPs were to reach the heart they could conceivably cause ischemia, contributing to adverse cardiovascular events. In ischemic myocardium, disrupted adherens junctions are associated with mislocalized gap junction plaques (Matsushita et al., 1999). Gap junctions ensure action potential propagation, however, improperly localized gap junctions result in arrhythmias (Peters et al., 1997; Shaw and Rudy, 1997; Kaprielian et al., 1998).

The DEP concentrations used in the *in vitro* experiments are likely higher than actual inhaled levels of DEPs. To date, *in vivo* concentrations of inhaled DEP reaching endothelial surfaces cannot be measured. Even an estimate would require consideration of inhalation capacity, the site and rate of DEP deposition, particle size distribution, efficiency of clearance, and transmigration of the particles through the alveolar membranes to the capillary endothelial cells. However, concentrations of DEPs reaching certain areas in the lung may be variable, and in some alveolar locations concentrations may approach our lowest *in vitro* concentration. Whether or not the concentrations are biologically relevant, the data do show proof of principle, demonstrating that a 24 h exposure to DEPs does, indeed, disrupt VE-cadherin in the adherens junctions of endothelial cells pre-assembled into tube networks, and that some particles do enter endothelial cells and the tubular lumen. While an *in vitro* system such as this cannot directly relate to the *in vivo* situation, the data presented do support the idea that if inhaled DEPs encounter alveolar endothelia, they may have a direct impact on the vascular cell–cell junctions and may translocate to the bloodstream.

Conflict of interest

The authors declare that there are no conflicts of interest.

Acknowledgements

Special thanks to Sarah Sparks, Sarah Hehir, and Dr. Kathryn Ulrich, Department of Chemistry, Rutgers University, for assistance with the light scattering experiments. Thanks to Dr. Gisela Witz for helpful discussions and critical reading of the manuscript.

This work was supported by the National Eye Institute (NEI) grant [EY009056] to MKG, the National Institute of Environmental Health Sciences (NIEHS) grant [ES13520] to RJL, the National Institutes of Arthritis and Musculoskeletal and Skin Disease (NIAMS) [U54AR055073] to the UMDNJ/Rutgers CounterACT Center of Excellence, and by the National Institute of Environmental Health Sciences (NIEHS) [P30ES005022] awarded to the UMDNJ/Rutgers Center for Environmental Exposures and Disease (CEED).

References

- Alexis, N.E., Lay, J.C., Zeman, K.L., Geiser, M., Kapp, N., Bennett, W.D., 2006. In vivo particle uptake by airway macrophages in healthy volunteers. *Am. J. Respir. Cell Mol. Biol.* 34, 305–313.
- Bai, Y., Suzuki, A.K., Sagai, M., 2001. The cytotoxic effects of diesel exhaust particles on human pulmonary artery endothelial cells in vitro: role of active oxygen species. *Free Radic. Biol. Med.* 30, 555–562.
- Baulig, A., Garlatti, M., Bonvallot, V., Marchand, A., Barouki, R., Marano, F., Baeza-Squiban, A., 2003. Involvement of reactive oxygen species in the metabolic pathways triggered by diesel exhaust particles in human airway epithelial cells. *Am. J. Physiol. Lung Cell. Mol. Physiol.* 285, L671–679.
- Brown, J.S., Zeman, K.L., Bennett, W.D., 2002. Ultrafine particle deposition and clearance in the healthy and obstructed lung. *Am. J. Respir. Crit. Care Med.* 166, 1240–1247.
- Corada, M., Mariotti, M., Thurston, G., Smith, K., Kunkel, R., Brockhaus, M., Lampugnani, M.G., Martin-Padura, I., Stoppacciaro, A., Ruco, L., McDonald, D.M., Ward, P.A., Dejana, E., 1999. Vascular endothelial-cadherin is an important determinant of microvascular integrity in vivo. *Proc. Natl. Acad. Sci. U.S.A.* 96, 9815–9820.
- Corada, M., Liao, F., Lindgren, M., Lampugnani, M.G., Breviario, F., Frank, R., Muller, W.A., Hicklin, D.J., Bohlen, P., Dejana, E., 2001. Monoclonal antibodies directed to different regions of vascular endothelial cadherin extracellular domain affect adhesion and clustering of the protein and modulate endothelial permeability. *Blood* 97, 1679–1684.
- Dales, R., Liu, L., Szyszkowicz, M., Dalipaj, M., Willey, J., Kulka, R., Ruddy, T.D., 2007. Particulate air pollution and vascular reactivity: the bus stop study. *Int. Arch. Occup. Environ. Health* 81, 159–164.
- Dejana, E., Orsenigo, F., Lampugnani, M.G., 2008. The role of adherens junctions and VE-cadherin in the control of vascular permeability. *J. Cell Sci.* 121, 2115–2122.

- Donovan, D., Brown, N.J., Bishop, E.T., Lewis, C.E., 2001. Comparison of three in vitro human 'angiogenesis' assays with capillaries formed in vivo. *Angiogenesis* 4, 113–121.
- Esser, S., Lampugnani, M.G., Corada, M., Dejana, E., Risau, W., 1998. Vascular endothelial growth factor induces VE-cadherin tyrosine phosphorylation in endothelial cells. *J. Cell Sci.* 111 (Pt 13), 1853–1865.
- Gallicano, G.I., Bauer, C., Fuchs, E., 2001. Rescuing desmoplakin function in extra-embryonic ectoderm reveals the importance of this protein in embryonic heart, neuroepithelium, skin and vasculature. *Development* 128, 929–941.
- Garcia, J.G., Dodson, R.F., Callahan, K.S., 1989. Effect of environmental particulates on cultured human and bovine endothelium. Cellular injury via an oxidant-dependent pathway. *Lab. Invest.* 61, 53–61.
- Geiser, M., Rothen-Rutishauser, B., Kapp, N., Schurch, S., Kreyling, W., Schulz, H., Semmler, M., Im Hof, V., Heyder, J., Gehr, P., 2005. Ultrafine particles cross cellular membranes by nonphagocytic mechanisms in lungs and in cultured cells. *Environ. Health Perspect.* 113, 1555–1560.
- Geiser, M., Casaulta, M., Kupferschmid, B., Schulz, H., Semmler-Behnke, M., Kreyling, W., 2008. The role of macrophages in the clearance of inhaled ultrafine titanium dioxide particles. *Am. J. Respir. Cell. Mol. Biol.* 38, 371–376.
- Gilliland, F.D., Li, Y.F., Saxon, A., Diaz-Sanchez, D., 2004. Effect of glutathione-S-transferase M1 and P1 genotypes on xenobiotic enhancement of allergic responses: randomised, placebo-controlled crossover study. *Lancet* 363, 119–125.
- Gotsch, U., Borges, E., Bosse, R., Boggemeyer, E., Simon, M., Mossmann, H., Vestweber, D., 1997. VE-cadherin antibody accelerates neutrophil recruitment in vivo. *J. Cell Sci.* 110 (Pt 5), 583–588.
- Grant, D.S., Lelkes, P.I., Fukuda, K., Kleinman, H.K., 1991. Intracellular mechanisms involved in basement membrane induced blood vessel differentiation in vitro. *In Vitro Cell Dev. Biol.* 27A, 327–336.
- Hadley, M.A., Byers, S.W., Suarez-Quian, C.A., Kleinman, H.K., Dym, M., 1985. Extracellular matrix regulates Sertoli cell differentiation, testicular cord formation, and germ cell development in vitro. *J. Cell Biol.* 101, 1511–1522.
- Inoue, K., Takano, H., Sakurai, M., Oda, T., Tamura, H., Yanagisawa, R., Shimada, A., Yoshikawa, T., 2006. Pulmonary exposure to diesel exhaust particles enhances coagulatory disturbance with endothelial damage and systemic inflammation related to lung inflammation. *Exp. Biol. Med.* 231, 1626–1632.
- Ito, T., Ikeda, M., Yamasaki, H., Sagai, M., Tomita, T., 2000. Peroxynitrite formation by diesel exhaust particles in alveolar cells: links to pulmonary inflammation. *Environ. Toxicol. Pharmacol.* 9, 1–8.
- Jaques, P.A., Kim, C.S., 2000. Measurement of total lung deposition of inhaled ultrafine particles in healthy men and women. *Inhal. Toxicol.* 12, 715–731.
- Kaprielian, R.R., Gunning, M., Dupont, E., Sheppard, M.N., Rothery, S.M., Underwood, R., Pennell, D.J., Fox, K., Pepper, J., Poole-Wilson, P.A., Severs, N.J., 1998. Down-regulation of immunodetectable connexin43 and decreased gap junction size in the pathogenesis of chronic hibernation in the human left ventricle. *Circulation* 97, 651–660.
- Kevil, C.G., Ohno, N., Gute, D.C., Okayama, N., Robinson, S.A., Chaney, E., Alexander, J.S., 1998. Role of cadherin internalization in hydrogen peroxide-mediated endothelial permeability. *Free Radic. Biol. Med.* 24, 1015–1022.
- Kevil, C.G., Okayama, N., Alexander, J.S., 2001. H₂O₂-mediated permeability II: importance of tyrosine phosphatase and kinase activity. *Am. J. Physiol. Cell. Physiol.* 281, C1940–1947.
- Kreyling, W.G., Semmler, M., Erbe, F., Mayer, P., Takenaka, S., Schulz, H., Oberdorster, G., Ziesenis, A., 2002. Translocation of ultrafine insoluble iridium particles from lung epithelium to extrapulmonary organs is size dependent but very low. *J. Toxicol. Environ. Health A* 65, 1513–1530.
- Kreyling, W.G., Semmler-Behnke, M., Seitz, J., Scymczak, W., Wenk, A., Mayer, P., Takenaka, S., Oberdorster, G., 2009. Size dependence of the translocation of inhaled iridium and carbon nanoparticle aggregates from the lung of rats to the blood and secondary target organs. *Inhal. Toxicol.* 21 (Suppl. 1), 55–60.
- Kumagai, Y., Arimoto, T., Shinyashiki, M., Shimojo, N., Nakai, Y., Yoshikawa, T., Sagai, M., 1997. Generation of reactive oxygen species during interaction of diesel exhaust particle components with NADPH-cytochrome P450 reductase and involvement of the bioactivation in the DNA damage. *Free Radic. Biol. Med.* 22, 479–487.
- Lei, Y.C., Hwang, J.S., Chan, C.C., Lee, C.T., Cheng, T.J., 2005. Enhanced oxidative stress and endothelial dysfunction in streptozotocin-diabetic rats exposed to fine particles. *Environ. Res.* 99, 335–343.
- Li, N., Wang, M., Oberley, T.D., Sempf, J.M., Nel, A.E., 2002. Comparison of the pro-oxidative and proinflammatory effects of organic diesel exhaust particle chemicals in bronchial epithelial cells and macrophages. *J. Immunol.* 169, 4531–4541.
- Lucking, A.J., Lundback, M., Mills, N.L., Faratian, D., Barath, S.L., Pourazar, J., Cassee, F.R., Donaldson, K., Boon, N.A., Badimon, J.J., Sandstrom, T., Blomberg, A., Newby, D.E., 2008. Diesel exhaust inhalation increases thrombus formation in man. *Eur. Heart J.* 29, 3043–3051.
- Matsunaga, T., Arakaki, M., Kamiya, T., Endo, S., El-Kabbani, O., Hara, A., 2009. Involvement of an aldo-keto reductase (AKR1C3) in redox cycling of 9,10-phenanthrenequinone leading to apoptosis in human endothelial cells. *Chem. Biol. Interact.* 181, 52–60.
- Matsushita, T., Oyama, M., Fujimoto, K., Yasuda, Y., Masuda, S., Wada, Y., Oka, T., Takamatsu, T., 1999. Remodeling of cell–cell and cell–extracellular matrix interactions at the border zone of rat myocardial infarcts. *Circ. Res.* 85, 1046–1055.
- Nel, A.E., Diaz-Sanchez, D., Ng, D., Hiura, T., Saxon, A., 1998. Enhancement of allergic inflammation by the interaction between diesel exhaust particles and the immune system. *J. Allergy Clin. Immunol.* 102, 539–554.
- Nemmar, A., Vanbilloen, H., Hoylaerts, M.F., Hoet, P.H., Verbruggen, A., Nemery, B., 2001. Passage of intratracheally instilled ultrafine particles from the lung into the systemic circulation in hamster. *Am. J. Respir. Crit. Care Med.* 164, 1665–1668.
- Nemmar, A., Hoet, P.H., Vanquickenborne, B., Dinsdale, D., Thomeer, M., Hoylaerts, M.F., Vanbilloen, H., Mortelmans, L., Nemery, B., 2002a. Passage of inhaled particles into the blood circulation in humans. *Circulation* 105, 411–414.
- Nemmar, A., Hoylaerts, M.F., Hoet, P.H., Dinsdale, D., Smith, T., Xu, H., Vermeylen, J., Nemery, B., 2002b. Ultrafine particles affect experimental thrombosis in an in vivo hamster model. *Am. J. Respir. Crit. Care Med.* 166, 998–1004.
- Nemmar, A., Hoet, P.H., Dinsdale, D., Vermeylen, J., Hoylaerts, M.F., Nemery, B., 2003. Diesel exhaust particles in lung acutely enhance experimental peripheral thrombosis. *Circulation* 107, 1202–1208.
- Nemmar, A., Hoylaerts, M.F., Nemery, B., 2006. Effects of particulate air pollution on hemostasis. *Clin. Occup. Environ. Med.* 5, 865–881.
- Nemmar, A., Al-Maskari, S., Ali, B.H., Al-Amri, I.S., 2007. Cardiovascular and lung inflammatory effects induced by systemically administered diesel exhaust particles in rats. *Am. J. Physiol. Lung Cell. Mol. Physiol.* 292, L664–670.
- O'Neill, M.S., Veves, A., Zanobetti, A., Sarnat, J.A., Gold, D.R., Economides, P.A., Horton, E.S., Schwartz, J., 2005. Diabetes enhances vulnerability to particulate air pollution-associated impairment in vascular reactivity and endothelial function. *Circulation* 111, 2913–2920.
- Oberdorster, G., Ferin, J., Lehnert, B.E., 1994. Correlation between particle size, in vivo particle persistence, and lung injury. *Environ. Health Perspect.* 102 (Suppl 5), 173–179.
- Oberdorster, G., Sharp, Z., Atudorei, V., Elder, A., Gelein, R., Kreyling, W., Cox, C., 2004. Translocation of inhaled ultrafine particles to the brain. *Inhal. Toxicol.* 16, 437–445.
- Peters, A., Dockery, D.W., Muller, J.E., Mittleman, M.A., 2001a. Increased particulate air pollution and the triggering of myocardial infarction. *Circulation* 103, 2810–2815.
- Peters, A., Frohlich, M., Doring, A., Immervoll, T., Wichmann, H.E., Hutchinson, W.L., Pepys, M.B., Koenig, W., 2001b. Particulate air pollution is associated with an acute phase response in men; results from the MONICA-Augsburg Study. *Eur. Heart J.* 22, 1198–1204.
- Peters, A., von Klot, S., Heier, M., Trentinaglia, I., Hormann, A., Wichmann, H.E., Lowel, H., 2004. Exposure to traffic and the onset of myocardial infarction. *N. Engl. J. Med.* 351, 1721–1730.
- Peters, N.S., Coromilas, J., Severs, N.J., Wit, A.L., 1997. Disturbed connexin43 gap junction distribution correlates with the location of reentrant circuits in the epicardial border zone of healing canine infarcts that cause ventricular tachycardia. *Circulation* 95, 988–996.
- Pope 3rd, C.A., Dockery, D.W., 2006. Health effects of fine particulate air pollution: lines that connect. *J. Air Waste Manage. Assoc.* 56, 709–742.
- Riedl, M., Diaz-Sanchez, D., 2005. Biology of diesel exhaust effects on respiratory function. *J. Allergy Clin. Immunol.* 115, 221–228.
- Rundell, K.W., Hoffman, J.R., Caviston, R., Bulbulian, R., Hollenbach, A.M., 2007. Inhalation of ultrafine and fine particulate matter disrupts systemic vascular function. *Inhal. Toxicol.* 19, 133–140.
- Sagai, M., Saito, H., Ichinose, T., Kodama, M., Mori, Y., 1993. Biological effects of diesel exhaust particles. I. In vitro production of superoxide and in vivo toxicity in mouse. *Free Radic. Biol. Med.* 14, 37–47.
- Schmelz, M., Franke, W.W., 1993. Complexus adherentes, a new group of desmoplakin-containing junctions in endothelial cells: the syndesmos connecting retothelial cells of lymph nodes. *Eur. J. Cell Biol.* 61, 274–289.
- Semmler, M., Seitz, J., Erbe, F., Mayer, P., Heyder, J., Oberdorster, G., Kreyling, W.G., 2004. Long-term clearance kinetics of inhaled ultrafine insoluble iridium particles from the rat lung, including transient translocation into secondary organs. *Inhal. Toxicol.* 16, 453–459.
- Shaw, R.M., Rudy, Y., 1997. Ionic mechanisms of propagation in cardiac tissue. Roles of the sodium and L-type calcium currents during reduced excitability and decreased gap junction coupling. *Circ. Res.* 81, 727–741.
- Shimada, A., Kawamura, N., Okajima, M., Kaewamatawong, T., Inoue, H., Morita, T., 2006. Translocation pathway of the intratracheally instilled ultrafine particles from the lung into the blood circulation in the mouse. *Toxicol. Pathol.* 34, 949–957.
- Singh, P., DeMarini, D.M., Dick, C.A., Tabor, D.G., Ryan, J.V., Linak, W.P., Kobayashi, T., Gilmour, M.I., 2004. Sample characterization of automobile and forklift diesel exhaust particles and comparative pulmonary toxicity in mice. *Environ. Health Perspect.* 112, 820–825.
- Spring, K.R., 1998. Routes and mechanism of fluid transport by epithelia. *Annu. Rev. Physiol.* 60, 105–119.
- Sumanasekera, W.K., Ivanova, M.M., Johnston, B.J., Dougherty, S.M., Sumanasekera, G.U., Myers, S.R., Ali, Y., Kizu, R., Klinge, C.M., 2007. Rapid effects of diesel exhaust particulate extracts on intracellular signaling in human endothelial cells. *Toxicol. Lett.* 174, 61–73.
- Taddei, A., Giampietro, C., Conti, A., Orsenigo, F., Breviaro, F., Pirazzoli, V., Potente, M., Daly, C., Dimmeler, S., Dejana, E., 2008. Endothelial adherens junctions control tight junctions by VE-cadherin-mediated upregulation of claudin-5. *Nat. Cell Biol.* 10, 923–934.
- Takenaka, S., Karg, E., Kreyling, W.G., Lentner, B., Moller, W., Behnke-Semmler, M., Jennen, L., Walch, A., Michalke, B., Schramel, P., Heyder, J., Schulz, H., 2006. Distribution pattern of inhaled ultrafine gold particles in the rat lung. *Inhal. Toxicol.* 18, 733–740.
- Venkiteswaran, K., Xiao, K., Summers, S., Calkins, C.C., Vincent, P.A., Pumiglia, K., Kowalczyk, A.P., 2002. Regulation of endothelial barrier function and growth

- by VE-cadherin, plakoglobin, and beta-catenin. *Am. J. Physiol. Cell. Physiol.* 283, C811–821.
- Villasante, A., Pacheco, A., Ruiz, A., Pellicer, A., Garcia-Velasco, J.A., 2007. Vascular endothelial cadherin regulates vascular permeability: implications for ovarian hyperstimulation syndrome. *J. Clin. Endocrinol. Metab.* 92, 314–321.
- Waldman, W.J., Kristovich, R., Knight, D.A., Dutta, P.K., 2007. Inflammatory properties of iron-containing carbon nanoparticles. *Chem. Res. Toxicol.* 20, 1149–1154.
- Wan, J., Diaz-Sanchez, D., 2007. Antioxidant enzyme induction: a new protective approach against the adverse effects of diesel exhaust particles. *Inhal. Toxicol.* 19 (Suppl 1), 177–182.
- Xiao, K., Garner, J., Buckley, K.M., Vincent, P.A., Chiasson, C.M., Dejana, E., Faundez, V., Kowalczyk, A.P., 2005. p120-Catenin regulates clathrin-dependent endocytosis of VE-cadherin. *Mol. Biol. Cell* 16, 5141–5151.
- Yamawaki, H., Iwai, N., 2006. Mechanisms underlying nano-sized air-pollution-mediated progression of atherosclerosis: carbon black causes cytotoxic injury/inflammation and inhibits cell growth in vascular endothelial cells. *Circ. J.* 70, 129–140.
- Zanobetti, A., Schwartz, J., 2005. The effect of particulate air pollution on emergency admissions for myocardial infarction: a multicity case-crossover analysis. *Environ. Health Perspect.* 113, 978–982.
- Zhou, X., Stuart, A., Dettin, L.E., Rodriguez, G., Hoel, B., Gallicano, G.I., 2004. Desmoplakin is required for microvascular tube formation in culture. *J. Cell Sci.* 117, 3129–3140.
- Zimrin, A.B., Villeponteau, B., Maciag, T., 1995. Models of in vitro angiogenesis: endothelial cell differentiation on fibrin but not matrigel is transcriptionally dependent. *Biochem. Biophys. Res. Commun.* 213, 630–638.